ACTIVE FIBRE COMPOSITES: SENSORS AND ACTUATORS FOR SMART COMPOSITES & STRUCTURES

X. Kornmann, C. Huber, M. Barbezat, and A.J. Brunner

Polymers/Composites Laboratory, Swiss Federal Institute for Material Testing and Research (EMPA)
Überlandstrasse 129 CH-8600 Dübendorf, Switzerland

ABSTRACT

Active fibre composites made of 250 μm diameter piezoelectric fibres embedded in an epoxy matrix and sandwiched between two screen-printed interdigitated electrodes have been successfully manufactured. Free strains up to 0.22 % representing developed stresses in the range of 40 MPa were obtained with the AFCs. Different factors influencing the actuation properties such as polarisation temperature and interdigital electrode spacing have been studied in order to optimise the performance of the AFCs. The acoustic emission (AE) sensor properties of AFCs, evaluated with impedance and sensitivity measurements, indicate that AFCs have resonance frequencies in a suitable range to detect AE signals (between 50 and about 300 kHz) and in some cases a higher sensitivity in the direction of the piezoelectric fibres. Easily integrable in composite laminates because of their flat geometries (~ 300 microns in thickness), AFCs present a large potential for smart structures as actuators but also as sensors.

1. INTRODUCTION

Active fibre composites (AFCs) are constituted of uniaxially oriented piezoceramic fibres embedded in a polymer matrix and sandwiched between two interdigitated electrodes (see Fig. 1) and were initially developed in the Active Materials and Structure Laboratory (AMSL) at the Massachusetts Institute of Technology [1]. Via the interdigitated electrodes, the piezoelectric fibres are polarised along their length. Their piezoelectric properties are hence mainly determined by the piezoelectric strain constant d_{33}, with an absolute value which is two times higher than the piezoelectric strain constant d_{31} exploited in most other piezoelectric devices. When an electric voltage is applied to the electrodes, the electric field generated through the fibres causes an extension of these fibres in the longitudinal direction.

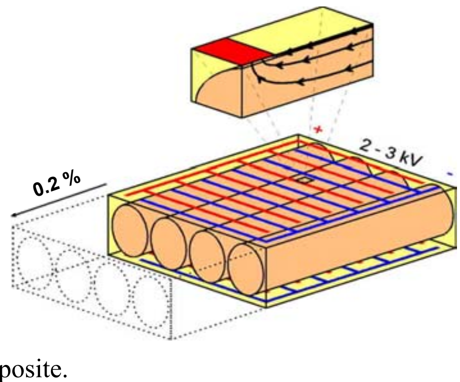

Fig. 1. Sketch of an active fibre composite.

These new composites can be used as sensors and actuators in smart composites and structures for health monitoring and active structural control, respectively and present major advantages over conventional piezoelectric materials. Their toughness and flexibility is superior to monolithic piezoceramics and their piezoelectric properties are better than those of piezopolymers like PVDF. Due to their high conformability and their increased piezoelectric performances, AFCs have been studied for active structural control of helicopter rotor [2], as well as devices for health monitoring of composite structures [3].

The present paper gives an overview of EMPAs research activities in the field of AFCs for active structural control and health monitoring (as sensor for acoustic emission). AFCs manufactured via a lamination process have been characterised as actuators and AE sensors in order to evaluate their potential for the development of smart composites and structures [4-7].

2. EXPERIMENTAL

Materials

Piezoelectric ceramic fibres PZT-5A with a diameter of ca. 250 microns (supplied by Smart Material Corporation, Osprey, USA) and polyimide foils of Kapton (100 HN, 25 microns in thickness supplied by Dupont, Mechelen, Belgium) were used for the preparation of the screen-printed electrodes. The silver paste used for the electrodes was the CB025 from Dupont. A two-component epoxy resin, Araldite LY 564/Aradur 2954 (Vantico AG, Basel, Switzerland), was used in combination with few drops of the antifoaming agent BYK-A530 (BYK-Chemie GmbH, Wesel, Germany) as matrix for the Active Fibre Composite.

Manufacture of the AFCs

Active Fibre Composites were manufactured according to a procedure similar to that described earlier by Bent [1]. A fibre mat was first prepared with the piezoelectric fibres in order to orient them parallel to one another. The fibre mat was then transferred between the interdigitated electrodes and the epoxy matrix was added (see Fig. 2). The AFC was contacted with cables and placed under a hydraulic press at 120°C. High pressure (ca. 25 bars effective) was used in order to maximise the contact angle between the fibres and the interdigitated electrodes.

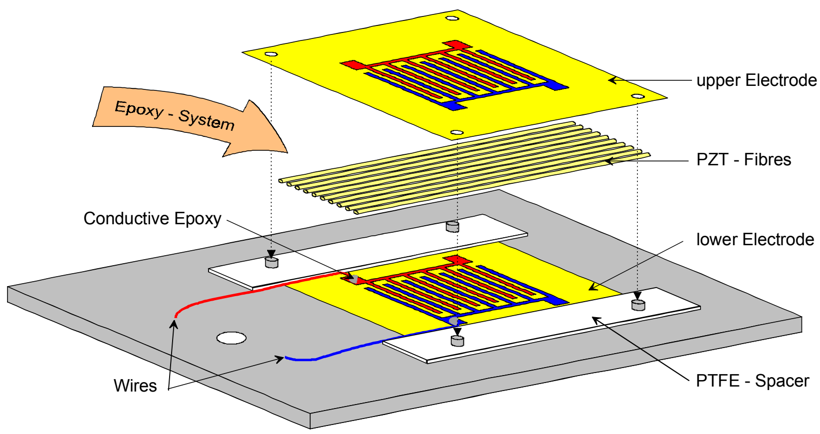

Fig. 2. Lamination of an active fibre composite.

The AFC was cured for 1 hour at 120°C and post cured for 8 hours at 160°C. All AFCs were poled with an electrical voltage of 2.8 kV/mm in an oven at 80°C for 20 minutes. The dimensions of the AFCs were: 31 mm in length, 20 mm in width (active area) and approximately 310 μm in thickness. The electrode finger width was 200 μm and the finger spacings were 700 μm, 900 μm, 1100 μm, or 1300 μm depending on the type of the AFC.

Free strain measurements

The free strain of AFCs was measured with standard 350 ohm electrical resistance foil strain gauges (Type 1-LY11-10/350 supplied by HBM AG, Nänikon, Switzerland) bonded symmetrically on both sides of the AFCs and connected in series to an amplifier via a half Winston bridge. Connecting each symmetric strain in series eliminates measurement errors linked to an eventual bending of the actuator during the test. Electric fields between –3 and +3 kV/mm were applied to the AFCs. The longitudinal free strain of the AFCs was recorded to generate characteristic actuation curves (i.e., butterfly or work cycle), which are the results of three consecutive cycles.

Tensile tests

AFCs for tensile testing had the following dimensions: 20 mm in width and 150 mm in length and were manufactured identically to the other AFCs. Glass fibre/epoxy tabs of dimensions 20 mm x 25 mm were glued at each extremities with Araldite epoxy glue. HBM strain gauges identical to the one used for the free strain measurements were glued symmetrically on both sides of the specimens. The tensile tests were conducted on an Instron 1251 hydraulic test machine with a 10 kN load cell at an extension rate of 0.3 mm/min.

Impedance measurements

An impedance analyser (Hewlett Packard HP 4194A) was used to measure the electrical impedance of different AFCs directly. At each frequency, the analyser measured both the voltage and current and computed their ratio, which (in the absence of cabling effects) is just the transducer electrical input impedance. The transducer was connected to the analyser through a 16047D test fixture and short wires. The analysis of the impedance measurements was performed between 100 Hz and 300 kHz.

Acoustic emission measurements

AE measurements with conventional AE sensors have been performed in parallel with those using the AFC elements. Standard 150 kHz resonant sensors (type SE-150M from Dunegan Engineering Corporation Inc., diameter 20.5 mm, height 14 mm, total weight 12 g including case) have been used in the comparison. An AMS-3 instrument and software (Vallen Systeme GmbH, Icking, Germany) was used for the AE signal acquisition and analysis. Detection thresholds were set at 40 dB, preamplifier gain at 34 dB and rearm time at 3.28 ms. A silicon-free vacuum grease was used as coupling agent; the AE sensors were mounted with spring clamps, and the AFC elements with scotch tape. The signals generated by the AFC elements have been registered and analysed with the AE equipment (via the AE preamplifiers and using the same data acquisition settings as for the AE sensors). Hsu-Nielsen sources, i.e., pencil lead breaks (see, e.g. [8] for details) provided simulated AE signals for verification of the coupling and sensitivity of both types of sensors.

In the polar diagrams, the AE sensors and AFCs were mounted on a polymethylmethacrylate (PMMA) plate and their signals were treated with either 30-1'000 or 95-1’000 kHz band pass filters.
The frequency spectrum of the pencil lead breaks was evaluated with a flat response (30 – 270 kHz) AE displacement sensor (type SE1000-H) on the same PMMA plate.

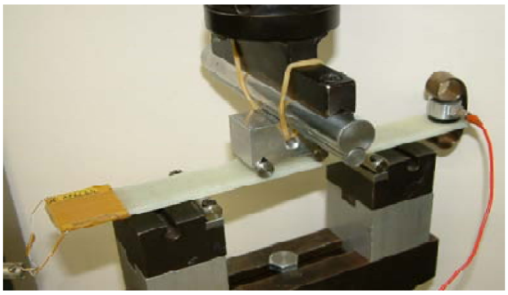

Fig. 3. Experimental set-up for the four-point bending test monitoring a glass fibre/epoxy beam with mounted AFC element (on the left) and AE sensor (on the right).

The quasi-static short-term four-point bending tests were performed on specimens (250 mm x 25 mm x 4.5 mm) cut out from a 0/90°-glass fibre fabric reinforced plastic (GFRP) laminate (Fig. 3). The four-point bending test procedure was derived from the EN ISO 14’215 standard using a lower span of 102 mm and an upper span of 34 mm. A constant displacement rate of 5 mm/min was applied. The specimens had 74 mm overhang on both sides in order to bond an AFC sensor on one end and to mount one AE sensor on the other. The aim of these tests was to investigate the potential of the AFC elements for damage detection in composite laminates in comparison with AE sensors.

3. RESULTS & DISCUSSION

Active structural control

Free strain measurements

Influence of the polarisation temperature

Fig. 4 presents free strain curves obtained by applying an electric field varying between –3 and +3 kV/mm. These so-called butterfly curves are characteristic of piezoelectric materials and yield valuable indications of the state of polarisation of the piezoelectric fibres.

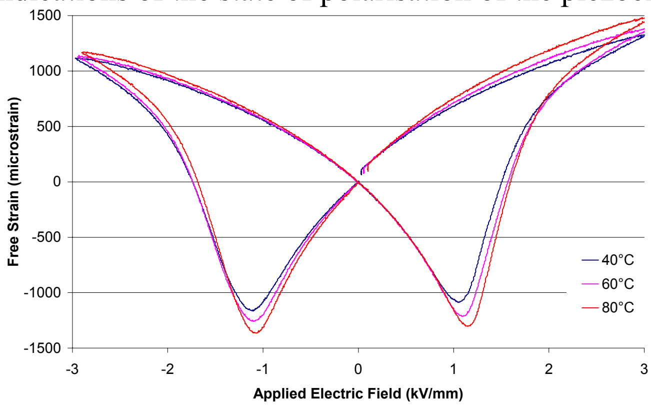

Fig. 4. Influence of different polarisation temperatures (40°C, 60°C, and 80°C) on the butterfly curves of active fibre composites.

Until now, butterfly curves have been generated with 1-3 composites [9] and it is interesting to see that a similar characterisation can also be performed with AFCs. It is clear from this figure that increasing the poling temperature from 40°C to 80°C improves the free strain performance of the AFCs. This is due to the fact that the mobility of dipoles in piezoelectric materials is favoured at higher temperatures. The coercitive field E_c, which corresponds to the electric field where dipole inversion takes place, increases from 1.08 to 1.18 kV/mm as the poling temperature increases from 40°C to 80°C.

Influence of the interdigital electrode spacing

Another approach to improve the free strain of active fibre composites is to increase the interdigital electrode spacing as shown in Fig. 5. Interestingly, increasing the interdigital electrode spacing and therefore the voltage necessary to generate the same applied electric field by 53 % (from 0.7 mm to 1.3 mm), increases the maximal free strain by only 10 % (from 2000 to 2200 microstrain). This improvement can be explained by the more uniform electric field generated along the piezoelectric fibres as the interdigital electrode spacing increases (see electric field profile in the fibres presented in Fig. 1). The major drawback of this parameter optimisation is the fact that the larger applied voltage required to drive the AFCs is increasing the risk of electrical breakdown within the composite.

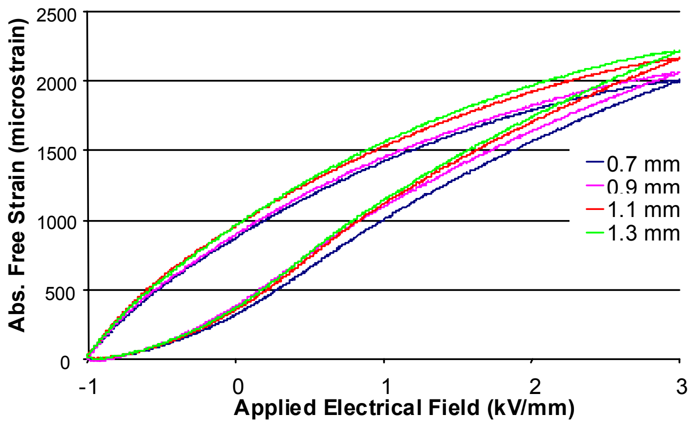

Fig. 5. Influence of the interdigital electrode spacing (0.7 mm, 0.9 mm, 1.1 mm, and 1.3 mm) on the work cycle of active fibre composites (absolute free strain).

Stress measurements

While free strain measurements are very useful for the characterisation and the optimisation of AFCs, the evaluation of the mechanical stress developed by these new actuators is very important for their applications in the field of active structural control. However, a direct evaluation of the mechanical stresses developed is difficult due to the small strains involved (typically less than 0.2%). An indirect method conventionally used consists of gluing the actuator on a metal strip, measuring the bending of the strip when the AFC is activated and then back-calculating the stress developed with a simple analytical model. The problems of this characterisation method are that the results do depend on the properties of the glue and the validity of the hypotheses made in the analytical model.
Another method consists of first establishing the work cycle of the AFC as presented in Fig. 5. Then it is possible to perform a tensile test on the same sample in order to obtain a stress

strain-curve of the active fibre composite (see Fig. 6a). Finally, if the data obtained from the work cycle and from the stress-strain curve are combined, it is possible to plot the estimated mechanical stress developed by the actuators as a function of applied electric field (see Fig. 6b).

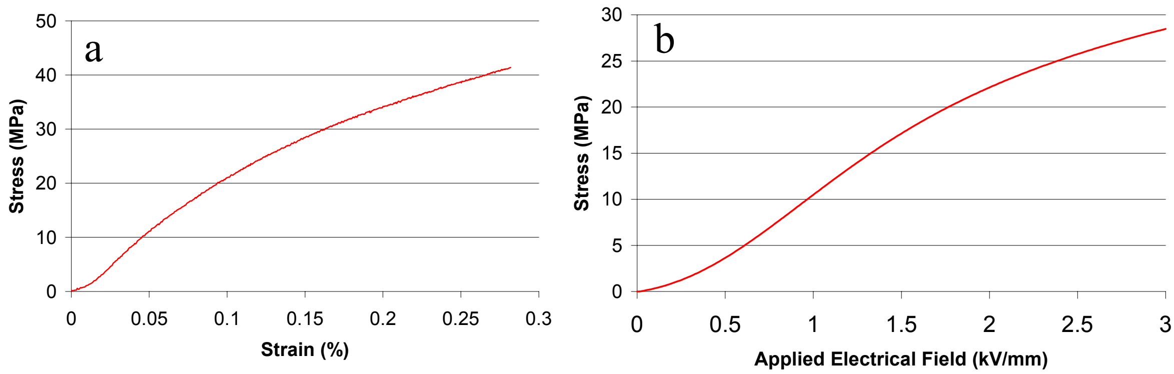

Fig. 6. Stress-strain behaviour of an active fibre composite (a) and estimated mechanical stress developed as a function of applied electric field (b).

Fig. 6a shows that similarly to tensile tests performed previously on single piezoelectric fibres [4], the stress-strain behaviour of AFCs is non-linear. The stress-applied electric field curve presented in Fig. 6b is therefore the combination of two non-linear curves (work cycle and stress-strain curves). The maximum stress developed by the AFC with varying the applied electric field from 0 to 3 kV/mm is almost 30 MPa. Varying the applied electric field from –1 to +3 kV/mm would increase the maximum stress by ca. 30 % (i.e. ca. 40 MPa).

Acoustic emission monitoring

Impedance measurements

Fig. 7a presents the results of the impedance measurements for AFCs with different interdigital electrode spacing. The variation of the phase angle theta indicates that resonance frequencies of the AFCs occur at 50, 135 and 225 kHz. The intensity of the different peaks increases with the interdigital electrode spacing but the frequency of the peaks remains essentially unchanged.

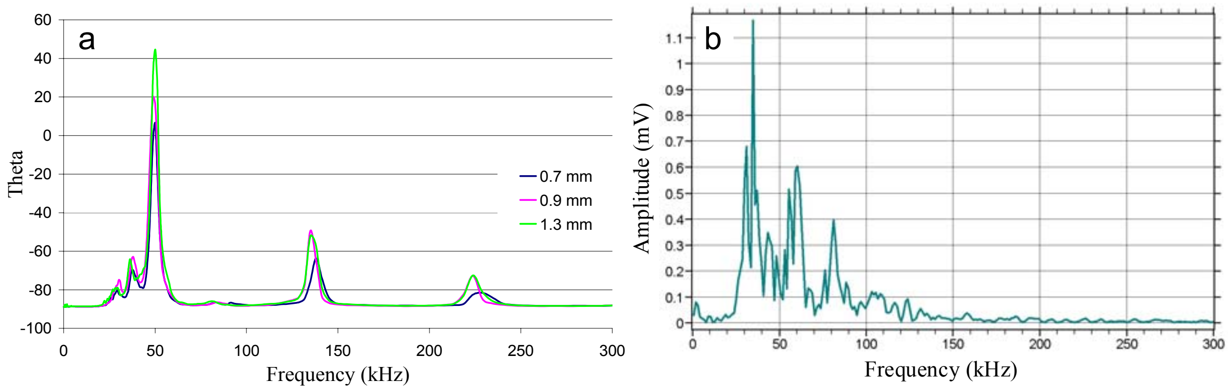

Fig. 7. Impedance measurements of AFCs with different interdigital electrode spacing (a) and frequency spectrum of a pencil lead break detected by a broad band AE sensor 20 cm from the source on a PMMA plate (b).

Fig. 7b shows the frequency spectrum of a pencil break detected by a flat response displacement AE sensor on a PMMA plate (simulated signal at a distance of 20 cm from the centre of the sensor). Interestingly, the frequency range of the signal matches well with the first resonance frequency of the AFC at 50 kHz. This could explain why AFCs are particularly sensitive to AE signals.

Polar diagrams

Fig. 8 presents a polar plot of sensitivities for simulated AE signals recorded by AE and AFC sensors on a PMMA plate when the sensor output signals are filtered with 30 and 95 kHz band-pass filters, respectively. Standard 150 kHz resonant AE sensors (blue squares) show an isotropic sensitivity response independent of the type of filter used. In contrast, AFC sensors present different responses depending on the filter used (red triangles). Thus, with the 30 kHz filter, the AFC sensitivity is isotropic and similar to that of the standard AE sensor. However, when the 95 kHz filter is used, the sensitivity decreases and the sensitivity pattern becomes, interestingly, anisotropic. The AFC response is then higher in the direction of the piezoelectric fibres than perpendicular to them. Apparently, eliminating the frequency range of 30-95 kHz corresponding to the main resonance peak of the AFC (see Fig. 7a) is responsible for this effect. These results suggest that the main resonance peak at 50 kHz is responsible for the isotropy of the AFC sensitivity.

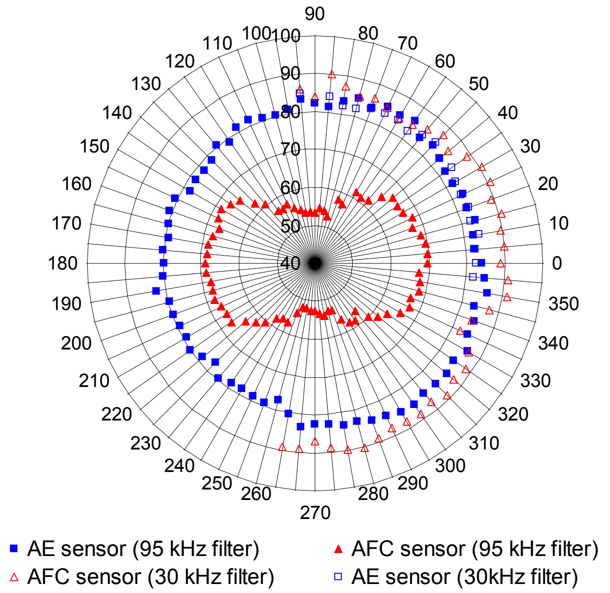

Fig. 8. Polar plot of sensitivity (average amplitude of three pencil lead breaks in dB at each location) both for AE sensor SE-150M (blue squares) and AFC elements (red triangles) on a PMMA-plate (simulated AE signals at a distance of 20 cm from the centre of the sensor). The fibres of the AFC elements are parallel to the 0°-to-180°-axis. The open and closed symbols indicate measurements with 30-1000 and 95-1000 kHz band pass filters, respectively.

These results are particularly interesting since filtering the AFCs output at different frequency thresholds permit to use the latter alternatively as isotropic or anisotropic sensors. The use of anisotropic sensors can be interesting, for instance, to compensate the anisotropic signal attenuation induced by preferred fibre orientations in composite laminates.

Acoustic emission monitoring

Fig. 9 presents the results of the the four-point bending test monitoring a glass fibre/epoxy beam with mounted AFC element and AE sensor on each extremities of the beam (see Fig. 3). The events detected by both sensors correspond to cracks and delamination growth in the glass fibre/epoxy beam. As the load level approaches the average failure load, the number of these events increases dramatically. This experiment was carried out with the 95-1’000 kHz band-pass filter. Due to the lower sensitivity of the AFC when this filter is used, the number of events detected by the AFC is lower than that measured by the conventional AE sensor. However, this experiment demonstrates that AFCs can be used as AE sensors to detect the appearance of defects in composite structures. It has been shown (see [5] for details) that both types of sensor yield a comparable assessment of the structural integrity of the GFRP-beam in these tests. The next step would be to repeat the experiments with the 30-1’000 kHz filter since we know from Fig. 8 that with this filter the sensitivity of AFCs is similar to standard AE sensors.

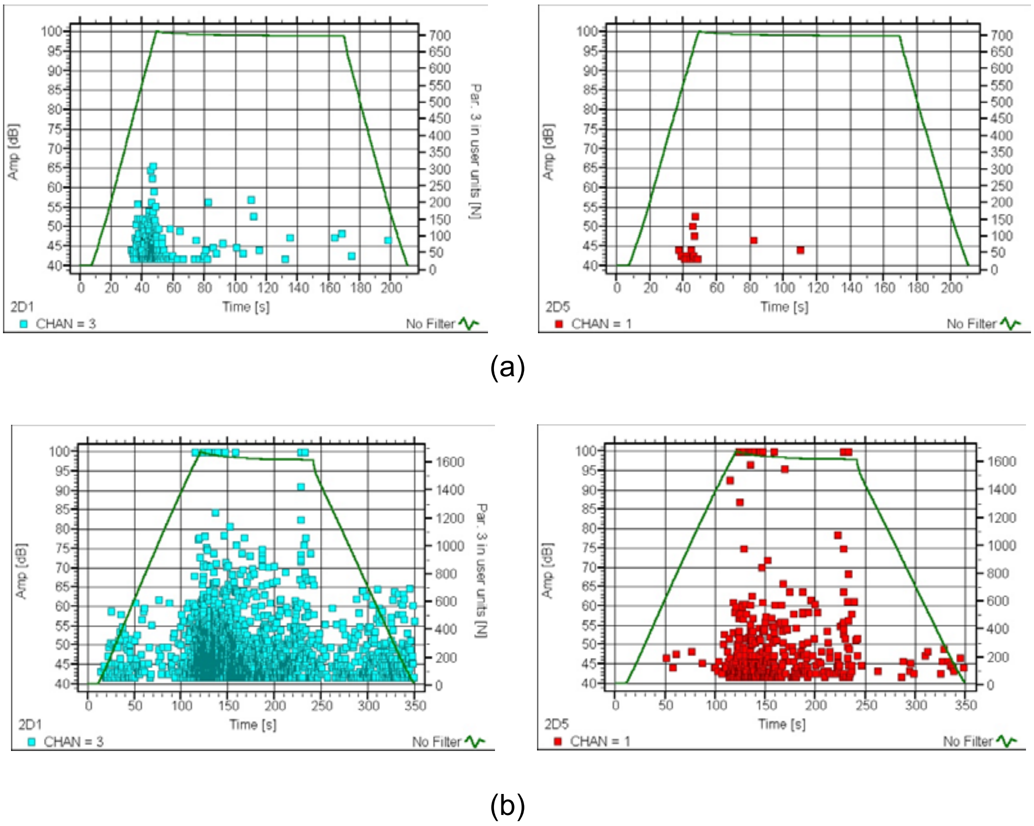

Fig. 9. Amplitude distribution for 2 load levels (40 % (a) and 95 % (b) of average failure load) from the four-point bending test on a GFRP-beam for the AE sensor (left) and the AFC (right). The green line indicates the load pattern.

4. CONCLUSIONS

Active Fibre Composites manufactured at EMPA may be used as actuator for active structural control or as AE sensor for structural health monitoring. Free strains up to 0.22 %

representing developed stresses of ca. 40 MPa can be generated by these AFCs. Increasing the polarisation temperature or the interdigital electrode spacing improves the free strain performance of AFCs. Alternatively, AFCs can also be efficiently used to replace conventional acoustic emission sensors. Easily integrable in composite structures, their sensitivity is in some cases at least comparable to that of standard AE sensors. Additionally, they can be used either as isotropic or anisotropic senors depending on the type of band pass filter used. Due to their actuator/sensor properties and their unusual conformability, AFCs show considerable potential for the development of the next generation of smart structures.

References

1. **Bent, A.** and **Hagood, N.W.**, „Piezoelectric fiber composites with interdigitated electrodes", *J. Intell. Mater. Syst. Struct.,* **8** (11) (1997), 903-919.¨

2. **Hall, S.R.** and **Prechtl, E.F.**, „Development of a piezoelectric servoflap for helicopter rotor control", *Smart Mater. Struct*., **5** (1996), 26-34.

3. **Datta, S.**, **Kirikera, G.R.**, **Schultz, M.J.**, and **Sundaresan, M.J.**, „Continuous sensors for structural health monitoring", *SPIE Conf. Proc., Smart Structures and Materials, San Diego March 2-6th,* **5046** (2003), 164-175.

4. **Kornmann, X.** and **Huber, C.,** „Microstructure and mechanical properties of PZT fibres*", J. Eur. Ceram. Soc.*, **24** (2004) 1987-1991.

5. **Barbezat, M., Brunner, A.J., Flüeler, P., Huber, C.,** and **Kornmann, X.,** „A comparison between active and passive piezoelectric elements for damage detection in fiber-reinforced composite laminates, *ATEM'03, JSME-MMD, Sep. 10-12* (2003).

6. **Barbezat, M., Brunner, A.J., Flüeler, P., Huber, C.,** and **Kornmann, X.,** „Acoustic emission sensor properties of active fibre composite elements compared with commercial acoustic emission sensors", *Sensors & Actuators A,* accepted for publication

7. **Kornmann, X., Huber, C.,** and **Elsener, H.-R.**, Piezoelectric ceramic fibers for active fiber composites: a comparative study, *SPIE Conf. Proc., Smart Structures and Materials, San Diego March 2-6th,* **5056** (2003), 330-337.

8. American Society for Nondestructive Testing (ASNT), *Handbook of Nondestructive Testing*, Vol. 5 Acoustic Emission Testing, 2nd Ed. (1987).

9. **L.J. Nelson, C.R. Bowen, R. Stevens, M. Cain,** and **M. Stewart**, „High field behaviour of piezoelectric fibre composites", *SPIE Conf. Proc., Smart Structures and Materials, San Diego, March 2-6th* , **5053** (2003) 544-555.